IEEE Access
Multidisciplinary | Rapid Review | Open Access Journal

Received 28 October 2022, accepted 5 December 2022, date of publication 20 December 2022, date of current version 3 January 2023.

Digital Object Identifier 10.1109/ACCESS.2022.3231158

RESEARCH ARTICLE

Trading Off Environmental and Economic Scheduling of a Renewable Energy Based Microgrid Under Uncertainties

RAHEEL ZAFAR[1], (Member, IEEE), ALI ESMAEEL NEZHAD[2], (Graduate Student Member, IEEE), ABDOLLAH AHMADI[3], (Member, IEEE), TOHID ERFANI[4], AND RASOOL ERFANI[4,5]

[1]Department of Electrical Engineering, Lahore University of Management Sciences, Lahore 54792, Pakistan
[2]Department of Electrical Engineering, School of Energy Systems, LUT University, 53850 Lappeenranta, Finland
[3]School of Electrical Engineering and Telecommunications, University of New South Wales, Sydney, NSW 2052, Australia
[4]Department of Civil, Environmental and Geomatic Engineering, University College London, WC1E 6BT London, U.K.
[5]Department of Engineering, Manchester Metropolitan University, M1 5GD Manchester, U.K.

Corresponding author: Ali Esmaeel Nezhad (ali.esmaeelnezhad@lut.fi)

ABSTRACT Smart power grids are transitioning towards effective employment of distributed energy resources including renewable energy sources to address the growing environmental concerns related to the pollutant emissions of fossil fuels. In this context, this paper proposes the directed search domain (DSD) method to compute the combined environmental and economic dispatch in a microgrid with battery energy storage systems, photovoltaic plants, wind turbines, fuel cells, and microturbines. The DSD algorithm is implemented for a multiobjective problem to obtain evenly-distributed Pareto optimal points by shrinking the original search domain into hypercone. This paper computes the optimal unit commitment and the related power dispatch while simultaneously minimizing the total pollutant emissions and operating costs. The best trade-off solution among the entire set of Pareto optimal points is computed by using the Fuzzy satisfying technique. The uncertainties associated with the forecasting of prices, load demand, wind, and photovoltaic power outputs are accounted for by employing the stochastic programming. The empirical results indicate the potential of the presented DSD algorithm in terms of the objective values, solution times, and quasi-even distribution of the Pareto set.

INDEX TERMS Directed search domain method, environmental/economic dispatch, fuzzy decision making, multiobjective optimization, renewable energy based microgrid, stochastic programming.

I. INTRODUCTION

Distributed generation (DG) is described as the small-scale production units supplying electricity to the consumers in close proximity to the generating units [1]. The presence of different kinds of energy sources such as wind turbines (WTs), photovoltaic (PV) plants, fuel cells (FCs), and microturbines (MTs) makes the concept of distributed generation more interesting [2]. The renewable energy sources (RESs) are the most popular and widely used DG units due to being sustainable, environment friendly, and free energy sources. Dispersed energy storage devices including battery (BA) storage systems are fundamental to the effective use of DG units as they help cope with the energy balance [2], [3]. The secure operation of power grids becomes overly complicated because of the intermittent nature of renewable energy sources including WTs and photovoltaic plants [4]. The integration of DG resources including the renewable energy sources into the smart grids can be realized by a subsystem known as microgrid (MG) [5]. The distributed generation, energy storage, and interconnected loads operate as a single controllable entity within microgrid framework. A point of common coupling (PCC) is the interconnecting point between power grid and microgrid. The microgrid is

The associate editor coordinating the review of this manuscript and approving it for publication was Chenghong Gu.

centrally managed by microgrid central controller (MGCC) that operates it in grid-connected mode during normal conditions and island mode during emergency conditions [6]. The microgrid is a promising concept with the potential of overcoming the challenges faced during the integration of intermittent RESs [5], [7].

A large amount of literature has considered the optimal operation of microgrids considering different control assets and loading conditions. Most researchers have focused on the economic dispatch of generating units to reduce cost or maximize profit. Reference [8] computed the power dispatch of storage system to minimize the cost of energy by using a microgrid controller. In [9], price signals ensured a balance between load and energy through the microgrid economic dispatch model. Reference [10] minimized the cost of total generation by computing the optimal dispatch of energy resources using a consensus-based distributed economic dispatch control method. Similarly, a microgrid operating in island mode employed the consensus approach presented by [11] to compute the solution of an economic dispatch problem. Reference [12] reduced the total operating cost by formulating a day-ahead scheduling problem of a power grid where energy storage systems, renewable energy sources, and conventional generating units were present. Reference [13] considered the plug-in electric vehicle as an energy storage in the renewable energy based microgrid. The objective was to reduce the cost through local production and generate revenue by exchanging the surplus energy with the utility grid considering the market price. The microgrid comprised of WTs, MTs, and FCs. All the studies reviewed above focus only on the economic aspect of microgrid operation while ignoring the issue of greenhouse gas emissions. The growing global commitments towards environmental protection such as the Net Zero by 2050 roadmap from International Energy Agency (IEA) necessitate the inclusion of emissions either as an objective function or as a constraint in the traditional economic dispatch problem [14], [15].

The combined environmental and economic dispatch (EED) problem computes the power dispatch of DG units while reducing the pollutant emissions along with the total operating cost. The EED problem is ideally casted as a multiobjective optimization model that mainly focuses on the simultaneous reduction of emission and cost objectives. In the multiobjective optimization problem, the competing nature of objective functions produces non-dominated solutions i.e., Pareto optimal points instead of unique solution [16]. A Pareto optimal solution cannot improve an objective without deteriorating the quality of at least one of the remaining objectives [17]. The surface formed within the objective space by Pareto optimal points is known as Pareto frontier. The large and growing body of the literature has solved the EED problem using evolutionary algorithms as well as classical mathematical programming approaches. Reference [18] reduced the emission and cost simultaneously in a renewable energy based microgrid using the adaptive modified particle swarm optimization algorithm (PSO). Likewise, the Fuzzy self-adaptive PSO method for the EED problem was presented in [19] to compute power dispatch of PV plants, WTs, MTs, BA, and FCs. Reference [20] proposed a reinforcement learning based on non-dominated sorting genetic algorithm (NSGA-RL) to concurrently optimize the emissions and cost in a power grid with wind turbines. Reference [21] converted the multiobjective EED model into a single-objective model through price penalty factor. The resultant single-objective problem was solved by using the differential evolution-crossover quantum PSO algorithm. It is pertinent to mention that the aforementioned metaheuristic methods are flexible and generally attain good solutions but these algorithms normally lack the theoretical guarantee for obtaining the global optimal solution. Moreover, the necessity to generate a huge number of solutions for well-representation of Pareto frontier may become an implementation barrier for these algorithms in practical scheduling problems with computational time constraints [16].

This paper aims to obtain evenly-distributed Pareto optimal points without generating a huge number of solutions to reduce the computational burden. The evenly-distributed Pareto set is of paramount importance as it aids the system operator to make a well-informed decision by analyzing only a very limited number of the Pareto optimal points. The generation of an evenly-distributed Pareto set necessitates the use of an algorithm with some sort of geometrical interpretation. The multiobjective EED problem has been solved extensively using evolutionary algorithms in the presence of forecasting uncertainties. Reference [22] employed lightning search algorithm (LSA) to solve the EED problem considering the load uncertainties and intermittent RESs. The system operator did not have the flexibility for trading off environmental and economic scheduling as the Pareto frontier was not formed in [22]. Reference [23] proposed a double deep Q-learning method to manage the operation of a multi-microgrid system considering the uncertainties in shortage/surplus power and market price signal. Here, the total operating cost was minimized without considering the reduction in the total pollutant emission. In [24], the EED problem was solved using the multiobjective antlion optimization (MALO) algorithm considering the uncertain nature of RESs and load demand. The Pareto optimal points for bi-objective optimization in [24] were not uniformly distributed over the Pareto frontiers. Reference [25] solved the EED problem using an improved multiobjective differential evolutionary (IMODE) optimization algorithm. Again, there is no guarantee of producing the quasi-evenly distributed Pareto set. In [26], the generation cost and pollutant emissions were reduced by using a grey wolf optimizer (GWO) algorithm while considering the forecasting uncertainties. The multiobjective algorithms in the above literature [22], [26] lack a geometrical interpretation, which is crucial for the generation of evenly-distributed Pareto optimal points.

The classical mathematical programming approaches commonly employ the weighted sum method to obtain a

single-objective optimization problem from the multiobjective EED problem. The linear combination of the objectives is described by weights that can be varied in multiple optimization runs to compute the Pareto optimal set. Reference [27] formulated a convex program to obtain the global optimum of the EED problem using the weighted sum approach combined with an analytical technique. Similarly, reference [28] presented a linear programming based outer approximation algorithm to compute the solution of the EED problem. Here, the piecewise linear functions were used to linearize the convex quadratic objective functions. In [29], the EED problem was solved by formulating a semidefinite program where the weighted sum method converted the vector objective into a scalar objective function. The evenly-distributed Pareto optimal points help to explore the entire Pareto frontier without the requirement of generating the large number of solutions. It is pertinent to mention that the weighted sum method lacks a geometrical interpretation and the weight coefficients are unknown function of the objectives. Moreover, the weight coefficients with an even distribution may not necessarily result in the Pareto optimal points with an even distribution [16].

The multiobjective optimization method with some sort of geometrical interpretation is an ideal candidate for the EED problem due to its potential to capture the entire Pareto frontier. Reference [30] optimized the generation cost, losses, and emissions in the power grids using the normal boundary intersection (NBI) method. Here, the best trade-off solution was determined by implementing a Fuzzy decision making method. The NBI method with a clear geometrical interpretation exhibits the capability of computing the evenly-distributed Pareto optimal points. Reference [31] generated evenly-distributed Pareto optimal points without requiring the objectives' scaling by proposing the NBI method to simultaneously minimize emissions and maximize profit. Also, the superiority of NBI method over weighted sum approach was established by generating the Pareto solutions with even-distribution. Note that the NBI method might be nonrobust as it reduces the feasible search domain to a line [16], [32]. The augmented epsilon-constraint technique has been proposed in [33] to reduce the emissions and cost in a renewable energy based microgrid. Compared to the weighted sum approach, the significant merits of epsilon-constraint method include the generation of non-extreme efficient solutions and absence of objectives' scaling requirement. It is pertinent to mention that the epsilon-constraint method lacks a clear geometrical interpretation and may not generate evenly-distributed Pareto optimal points, although its algorithm involves a payoff table with anchor points that are optima of each objective in the objective space. In [34], the normalized normal constraint (NNC) method is presented to minimize the economic and technical objectives including the microgrid operation cost. The NNC method, being a modification of NBI method, is more flexible with an ability to produce evenly-distributed Pareto optimal solutions due to its geometrical interpretation. However, both the NNC and NBI approaches may require filtering procedure as these methods have a potential to produce locally Pareto and non-Pareto solutions. This may render them inefficient in practical problems with computational time constraints as these methods may require the generation of a considerable amount of redundant solutions [16], [17].

The directed search domain (DSD) algorithm is an effective method to represent the well-distribution of Pareto optimal points over the whole Pareto frontier. The DSD algorithm has a clear geometrical interpretation and it was first suggested in [17] and [35] to produce the Pareto points with the quasi-even distribution. The DSD method computes a Pareto optimal point within a specific area of feasible objective space by shrinking the original search domain. Unlike the reduction of search domains into a set of rays by NBI method, the DSD algorithm shrinks the search domains into hypercones. This feature makes it more robust compared to NBI and NNC methods. Furthermore, the locally Pareto solutions can be easily filtered out and the DSD algorithm does not produce non-Pareto solutions [17]. Due to being a recently developed method for multiobjective optimization problems, there exists a relatively small body of literature concerned with the application of DSD algorithm in the area of power system operation. Reference [36] presented the enhanced DSD method to compute the optimal operation schedule in multi-carrier energy systems with conventional and renewable generating units. Similarly, the DSD algorithm was proposed in [37] to minimize the cost factor of wind farms as well as thermal units' generation cost in an optimal power flow problem. The preference criterion was defined to establish the superiority of DSD algorithm over augmented epsilon-constraint technique, weighted sum method, and NNC method.

In view of the above discussion, this paper addresses the concerns related to the uneven distribution of Pareto optimal points over the Pareto frontier in the combined environmental and economic dispatch problem. The optimal unit commitment and associated dispatch are determined while simultaneously reducing the total greenhouse gas emissions and operating cost. The microgrid consists of different conventional and renewable energy sources including MTs, FCs, WTs, and PV plants. The innovation and contributions of this paper are summarized as follows:

- A directed search domain algorithm is proposed to conduct the day-ahead environmental/economic scheduling in a renewable energy based microgrid. The DSD method with a geometrical interpretation computes quasi-evenly distributed Pareto set. To the best of authors' knowledge, this case study is the first implementation of DSD method for the multiobjective EED problem of a microgrid considering forecasting uncertainties.
- The detailed modeling of battery energy storage system is carried out to ensure the effective use of renewable energy based DG units. The impact of initial state-of-charge on the operation of battery storage is investigated. Also, the case study demonstrates the full satisfaction of battery storage constraints.

- The stochastic programming is implemented to account for the forecasting uncertainties related to the load demand, bid prices, WT's power output, and PV's power output. Most of the aforementioned studies have ignored the forecasting uncertainties in the microgrid scheduling problem. The modeling of forecasting uncertainties is executed by generating a significant amount of random scenarios. Afterwards, the backward scenario reduction algorithm is employed to decrease the total number of scenarios for establishing a trade-off between solution accuracy and computation burden [38].
- The best trade-off solution among all the Pareto optimal points is computed via Fuzzy satisfying technique. Compared to the approaches reported in the literature, the potential of the proposed DSD method in terms of objective values, solution times, and uniform distribution of Pareto set is indicated by the empirical results.

II. DAY-AHEAD OPERATION MODEL OF MICROGRID

The scenario-based stochastic bi-objective optimization framework is employed to model the environmental/economic scheduling problem of a microgrid. The objectives include the simultaneous reduction of total pollutant emissions and cost over the scheduling period.

A. TOTAL OPERATING COST MINIMIZATION

The total operating cost is the first objective function in a renewable energy-based microgrid denoted by F_1. Let $P(t, s, m)$ be the power generated by the mth microturbine at time instant t for scenario s. Define SDC_m and SUC_m as the shut-down and start-up costs of mth microturbine. The $\gamma(t, m)$ represents the price while the binary variable $\xi(t, s, m)$ describes the commitment status of mth microturbine. The amount of power exchanged with the upstream network is denoted by $P(t, g)$ and $\gamma(t, g)$ is the associated price. Let $\Omega_s(s = 1, \ldots, W)$ be the set of W initial scenarios, each with probability ρ_s. Here, a generic day-ahead scheduling problem is formulated where the scenario s changes its meaning depending on the context. In the deterministic model, the Ω_s becomes a singleton set comprising only the forecasted values with $\rho_s = 1$. In the stochastic model, the scenario s belongs to the uncertainty set Ω_s comprising random scenarios with associated probabilities. The total operating cost in €ct is mathematically expressed as (1a), shown at the bottom of the page.

The first row of (1a) describes the total operating cost of microturbines that consists of shut-down, start-up, and generation costs. Likewise, the total operating cost of BA, WTs, PV, and FCs is illustrated by rows 2-5, respectively. The last row indicates the total operating cost related to the exchange of power between microgrid and upstream network [18], [19]. In this paper, the equation (1a) is used by the case studies with bid prices information while (1b) is considered by the case studies with fuel cost coefficient data. Note that (1b) does not include the scenario representation as it is used only by the deterministic case study. The cost coefficients related to the fuel of ith thermal unit are illustrated by a_i, b_i, and c_i, where $i \in G$. Let $P(i)$ be the generated power of ith thermal generation unit. The quadratic cost function F_1 is given by [39] and [40]

$$F_1 = \sum_{i \in G} [a_i P(i)^2 + b_i P(i) + c_i] \tag{1b}$$

B. TOTAL POLLUTANT EMISSION MINIMIZATION

The total pollutant emissions is the second objective function denoted by F_2. Let $E_e(t, m)$ be the emission in kg/MWh for mth microturbine at time instant t with eth pollutant where $e \in ET$. This paper considers three important pollutants in the set ET: nitrogen oxides (NO_x), sulfur dioxide (SO_2), and carbon dioxide (CO_2). The total pollutant emission from microgrid and utility is mathematically expressed as [18] and [19]

$$F_2 = \sum_{s \in \Omega_s} \rho_s \sum_{t \in T} \sum_{e \in ET} \left\{ \begin{array}{l} \sum\limits_{b \in BA} P(t, s, b) * E_e(t, b) \\ + \sum\limits_{f \in FC} P(t, s, f) * E_e(t, f) \\ + \sum\limits_{m \in MT} P(t, s, m) * E_e(t, m) \\ + P(t, s, g) * E_e(t, g) \end{array} \right\} \tag{2a}$$

$$F_1 = \sum_{s \in \Omega_s} \rho_s \sum_{t \in T} \left\{ \begin{array}{l} \sum\limits_{m \in MT} SDC_m * [1 - \xi(t, s, m)] * \xi(t-1, s, m) + SUC_m * [1 - \xi(t-1, s, m)] * \xi(t, s, m) + P(t, s, m) * \gamma(t, m) \\ + \sum\limits_{b \in BA} SDC_b * [1 - \xi(t, s, b)] * \xi(t-1, s, b) + SUC_b * [1 - \xi(t-1, s, b)] * \xi(t, s, b) + P(t, s, b) * \gamma(t, b) \\ + \sum\limits_{w \in WT} SDC_w * [1 - \xi(t, s, w)] * \xi(t-1, s, w) + SUC_w * [1 - \xi(t-1, s, w)] * \xi(t, s, w) + P(t, s, w) * \gamma(t, w) \\ + \sum\limits_{p \in PV} SDC_p * [1 - \xi(t, s, p)] * \xi(t-1, s, p) + SUC_p * [1 - \xi(t-1, s, p)] * \xi(t, s, p) + P(t, s, p) * \gamma(t, p) \\ + \sum\limits_{f \in FC} SDC_f * [1 - \xi(t, s, f)] * \xi(t-1, s, f) + SUC_f * [1 - \xi(t-1, s, f)] * \xi(t, s, f) + P(t, s, f) * \gamma(t, f) \\ + P(t, s, g) * \gamma(t, g) \end{array} \right\} \tag{1a}$$

Note that the above formulation computes total emissions in kg by associating the emissions with power production from different energy sources. The case study with quadratic emission function can use F_2 in (2b). Again, the equation (2b) does not include the scenario representation as it is used only by the deterministic case study in this paper. Define emission coefficients of ith thermal unit as d_i, e_i, and f_i. The quadratic emission function F_2 is given by [39] and [40]

$$F_2 = \sum_{i \in G} [d_i P(i)^2 + e_i P(i) + f_i] \tag{2b}$$

C. POWER BALANCE CONSTRAINT

The proposed model does not permit any load curtailment and the entire load demand at each time instant t of the planning horizon needs to be strictly met; otherwise infeasibility occurs and the solution does not converge. Let $Load(t, s)$ denote the total load demand for scenario s at time instant t. The equality constraint (3a) forces the hourly aggregated power generation to exactly meet the hourly load demand of the microgrid.

$$\begin{aligned} &\sum_{b \in BA} P(t,s,b) + \sum_{w \in WT} P(t,s,w) + \sum_{p \in PV} P(t,s,p) \\ &\quad + \sum_{f \in FC} P(t,s,f) + \sum_{m \in MT} P(t,s,m) \\ &\quad + P(t,s,g) = Load(t,s) \end{aligned} \tag{3a}$$

The microgrid with few number of feeders usually has negligible power losses. Nevertheless, we can approximately compute the power loss P_{Loss} using B-loss coefficients in a typical 4-bus test network comprising thermal generation units. The total power generation should satisfy the total losses and load demand in such a situation. The power balance constraint related to the deterministic simulation study in Section V-A at a single time instant is given by

$$\sum_{i \in G} P(i) = Load + P_{Loss} \tag{3b}$$

The power production of thermal power plant ϕ is denoted by P_ϕ. The $BL_{\phi\varphi}$ is the (ϕ, φ) index entry of the B-loss coefficient matrix and N_{TP} describes the total number of thermal power plants. The loss as a function of generation units' output power is given by

$$P_{Loss} = \sum_{\phi=1}^{N_{TP}} \sum_{\varphi=1}^{N_{TP}} P_\phi \, BL_{\phi\varphi} \, P_\varphi \tag{4}$$

D. POWER LIMIT CONSTRAINTS

Let $PF_{MIN}(t, w)$ and $PF_{MAX}(t, w)$ be the minimum and maximum forecasted power output of the wth wind turbine, respectively. Define minimum and maximum power output of mth microturbine as $P_{MIN}(t, m)$ and $P_{MAX}(t, m)$, respectively. The power limit constraints on microgrid assets and upstream network are expressed as

$$\begin{cases} P_{MIN}(t,b) * \xi(t,s,b) \le P(t,s,b) \le P_{MAX}(t,b) * \xi(t,s,b) \\ PF_{MIN}(t,w) * \xi(t,s,w) \le P(t,s,w) \le PF_{MAX}(t,w) * \xi(t,s,w) \\ PF_{MIN}(t,p) * \xi(t,s,p) \le P(t,s,p) \le PF_{MAX}(t,p) * \xi(t,s,p) \\ P_{MIN}(t,f) * \xi(t,s,f) \le P(t,s,f) \le P_{MAX}(t,f) * \xi(t,s,f) \\ P_{MIN}(t,m) * \xi(t,s,m) \le P(t,s,m) \le P_{MAX}(t,m) * \xi(t,s,m) \\ P_{MIN}(t,g) \le P(t,s,g) \le P_{MAX}(t,g) \end{cases} \tag{5}$$

E. DETAILED BATTERY STORAGE MODELING

This subsection describes the detailed modeling of a battery storage system. Let $PCHA(t, s, b)$ and $PDIS(t, s, b)$ be the charging and discharging power of battery storage, respectively. The battery state-of-charge at time instant t is denoted by $SOC(t, s, b)$. The charging and discharging efficiencies are represented by η_b^{CHA} and η_b^{DIS}. The detailed battery storage model is given by [41]

$$\begin{aligned} SOC(t+1,s,b) &= SOC(t,s,b) + \Delta t \, [\eta_b^{CHA} * PCHA(t,s,b) \\ &\quad - PDIS(t,s,b)/\eta_b^{DIS}] && \text{(6a)} \\ SOC_{MIN}(t,b) &\le SOC(t,s,b) \le SOC_{MAX}(t,b) && \text{(6b)} \\ P(t,s,b) &= PDIS(t,s,b) - PCHA(t,s,b) && \text{(6c)} \\ SOC(25,s,b) &= SOC(1,s,b) && \text{(6d)} \\ 0 &\le PCHA(t,s,b) \le -P_{MIN}(t,b) \\ &\quad * \xi_{SIM}(t,s,b) && \text{(6e)} \\ 0 &\le PDIS(t,s,b) \le P_{MAX}(t,b) \\ &\quad * \{1 - \xi_{SIM}(t,s,b)\} && \text{(6f)} \end{aligned}$$

The constraint (6d) ensures the same initial and final state-of-charge. The binary variable $\xi_{SIM}(t, s, b)$ in (6e)-(6f) prevents the simultaneous charging and discharging operation of battery storage.

III. MULTIOBJECTIVE MATHEMATICAL PROGRAMMING AND SOLUTION METHODOLOGY

A generic form of multiobjective optimization model casted as a nonlinear vector optimization problem is described as

$$\begin{aligned} &\text{Minimize } F(x) = (F_1(x), F_2(x), \ldots, F_N(x))^T \\ &\text{subject to } x \in X^* \end{aligned} \tag{7}$$

where N denotes the total number of objectives, $F_i (i = 1, \ldots, N)$ refers to the ith objective function, and the vector x is in the feasible design space $X^* \in R^K$. The vector x^* defines the Pareto optimal solution while the vector $F(x^*)$ is the Pareto point [16]. The set $\{F(x) \mid x \in X^*\}$ defines the feasible objective space Z^*.

A. DIRECTED SEARCH DOMAIN METHOD

It is desirable to explore the entire Pareto frontier within the feasible objective space. An aggregate objective function (AOF) reduces the vector optimization problem into a scalar optimization problem by considering the linear combination of objective functions [17]. The evenly distributed

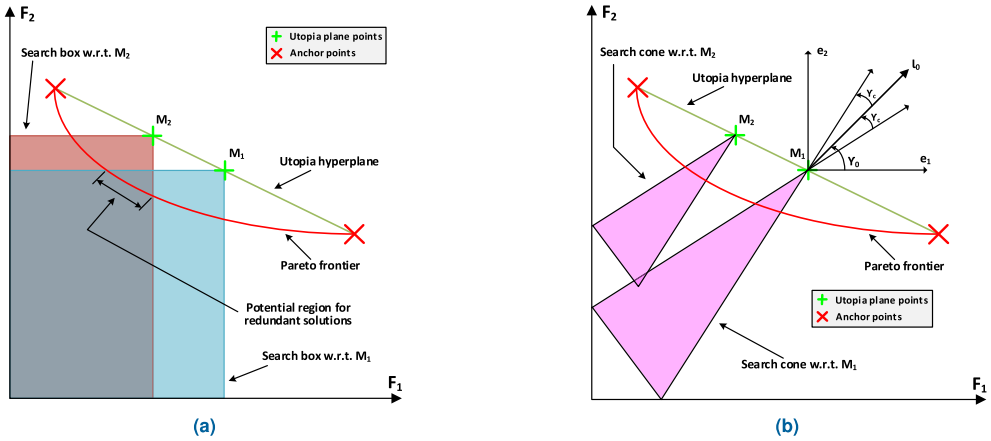

FIGURE 1. Generic two-dimensional case. (a) Objective space with initial search domain. (b) New search domain after shrinking using the proposed DSD algorithm.

Pareto optimal points may not be obtained by merely even spread of the weight coefficients in AOF [16]. The limitation of unevenly-distributed Pareto optimal points stems from its inability to capture the entire Pareto frontier. The well-representation of the whole Pareto frontier may not be possible without generating a huge number of solutions, which is computationally expensive. Only a very limited number of solutions can be considered by the decision maker due to the solution time constraints. Therefore, it is important to have a Pareto optimal set with the quasi-even distribution during the environmental/economic scheduling of the microgrid.

The DSD algorithm [17] explores the entire Pareto frontier. The DSD method shrinks the original search domain and computes a Pareto optimal point within the selected area of feasible objective space Z^*. The major steps involved in the DSD algorithm are described as [16] and [17]:

1. ***Generation of anchor points*** The anchor point μ_i corresponds to the optimum of an ith objective function. For illustration purposes, the two-dimensional case with anchor points in [16] is modified and depicted in Fig. 1. The case studies in Section V of this paper do not assume any preliminary scaling of objective functions.
2. ***Computation of evenly distributed utopia plane points*** All the anchor points in the feasible objective space Z^* are embedded in a hyperplane known as utopia hyperplane U. It can be mathematically given by

$$\begin{aligned} U &= \sum_{i=1}^{N} \lambda_i \mu_i \\ &\sum_{j=1}^{N} \lambda_j = 1 \\ &0 \le \lambda_i \le 1 \quad (i = 1, \ldots, N) \end{aligned} \tag{8}$$

The anchor points form the interior of the convex utopia polygon that carries the utopia plane points. The evenly distributed utopia plane points can be realized by uniformly varying the coefficients λ_i in (8). Note that the utopia plane points provide cheaply computed reference points similar to [42]. The light beam search concept combined with the even distribution of utopia plane points helps to explore the entire Pareto frontier.

3. ***Aggregate objective function (AOF)*** Although different aggregation techniques can be used that might reduce the computational effort, we use the simplest one as reported being effective for practical purposes in [16]. The case studies in Section V assume the AOF as the sum of the objective functions with equal weighting factors.
4. ***Shrinking of search domain*** Consider two objective functions F_1 and F_2 with a convex Pareto frontier. Define kth utopia plane point as $M_i^k (i = 1, \ldots, N; k = 1, .., N_U)$ where i denotes the coordinates of each utopia point and N_U is the total number of utopia plane points. The x and y coordinates of the kth utopia plane point M_1^k and M_2^k determine the upper bound for F_1 and F_2, respectively. The optimization problem of a generic N-dimensional case is formulated for the kth utopia plane point as [17]

$$\begin{aligned} &\text{Minimize} \sum_{i=1}^{N} F_i(x) \\ &\text{subject to } F_i \le M_i^k \quad \forall i \\ &x \in X^* \end{aligned} \tag{9}$$

The original search domain corresponding to each utopia plane point with $N = 2$ is depicted in Fig. 1(a). The optimization problem solved at different utopia points may generate redundant solutions due to the relatively large search domain as indicated by [17]. Fig. 1(a) clearly depicts the overlapping region on the Pareto frontier with the potential of producing the redundant solutions.

The DSD algorithm avoids generating redundant solutions by shrinking the search domain around a given direction as shown in Fig. 1(b). Different shrinking strategies are available (e.g., look at [32]). This paper considers the origin at each utopia plane point M^k for a Cartesian coordinate

system $e_i (i = 1, \ldots, N)$. Assume a unit vector $l_0 = (l_0, l_0, \ldots, l_0)^T$ that forms an angle γ_0 with the axes of Cartesian coordinate system so that $l_0 \equiv \cos\gamma_0 = 1/\sqrt{N}$. The case studies in Section V shrink the search domain around the unit vector l_0 as the shrinking of the search domain along the vector l_0 is usually sufficient. Note that the normal of the utopia hyperplane may not be parallel to the unit vector l_0 as illustrated in Fig. 1(b). Nevertheless, the reader may refer to the procedure described in [16] and [17] to realize a random direction of the search domain.

Consider an affine transformation denoted by $\hat{F}_i$ to represent the linear combination of all the available objective functions.

$$\hat{F}_i = \sum_{j=1}^{N} F_j D_{ji} \quad (\forall i = 1, \ldots, N) \tag{10}$$

Equation (11) determines the matrix D for the generic two-dimensional case with $N = 2$ and $\gamma_0 = 45^o$ where $\gamma_+ = \gamma_0 + \gamma_c$ and $\gamma_- = \gamma_0 - \gamma_c$.

$$D = \frac{1}{sin2\gamma_c} \begin{pmatrix} \sin\gamma_+ & -\sin\gamma_- \\ -\cos\gamma_+ & \cos\gamma_- \end{pmatrix} \tag{11}$$

Equation (10) being an affine transformation preserves the convexity. The affine transform is defined with an aim to localize the aggregate objective function around the vector l_0 by shearing the objective space. The constraint in (9) can be modified for the kth utopia point as follows:

$$\hat{F}_i \leq \sum_{j=1}^{N} M_j^k D_{ji} \quad (\forall i = 1, \ldots, N) \tag{12}$$

The optimization problem in (13) shrinks the original search box of Fig. 1(a) into the search cone of Fig. 1(b) at kth utopia plane point [16].

$$\begin{aligned} &\text{Minimize} \sum_{i=1}^{N} F_i(x) \\ &\text{subject to } \hat{F}_i \leq \sum_{j=1}^{N} M_j^k D_{ji} \quad (\forall i = 1, \ldots, N) \\ &\hat{F}_i = \sum_{j=1}^{N} F_j D_{ji} \quad (\forall i = 1, \ldots, N) \\ &x \in X^* \end{aligned} \tag{13}$$

The optimization problem in (13) results in the hypercone with its vertex at utopia point M^k as depicted in Fig. 1(b). A small enough value of angle γ_c ensures the quasi-even distribution of Pareto optimal points. It is apparent from the Fig. 1(b) that the redundant solutions are not possible due to the absence of the overlapping region.

5. ***Deterministic DSD model*** The sum of overall operating cost F_1 and total pollutant emission F_2 represents an AOF. The maximum amount of information about the Pareto frontier with the minimum computational burden is facilitated by a quasi-evenly distributed set of Pareto points [16]. In the deterministic model, the Ω_s becomes a singleton set comprising only the forecasted values with $\rho_s = 1$. The case study in Section V-A uses (3b) while the case studies in Sections V-B, V-C, and V-E employ (3a) as the power balance constraint. The proposed deterministic DSD model at the kth utopia point is given by

$$\begin{aligned} &\text{Minimize} \quad F_1 + F_2 \\ &\text{subject to} \quad (3), (5), (9)\text{-}(11). \end{aligned} \tag{14}$$

6. ***Limitations and assumptions of the proposed algorithm*** The proposed DSD algorithm with an angle γ_c in (11) determines the search cone that can be degenerated into a line when $\gamma_c \to 0$. In practical applications, an extremely small value of angle γ_c should be avoided as it might make the DSD algorithm nonrobust due to the degeneration of the feasible search cone into a line [17]. Also, the proposed DSD algorithm assumes the same number of objective functions and anchor points. Any violation of this assumption might lead to the degeneration of the convex utopia polygon formed by the anchor points [17], [32].

B. FUZZY SATISFYING TECHNIQUE

As previously described, the solution of a multiobjective optimization model may involve multiple optimal points, forming a set of optimal solutions, known as Pareto optimal points. The system operator should decide on the best Pareto solution, best fitting the operational strategy of the system. Hence, an efficient decision making technique must be deployed to pick the most desired solution. The Fuzzy satisfying method is regarded as one of the high-performance approaches to this end, having linear relationships [33], [43]. The structure of this approach is based on defining a linear membership function, assigned to each objective function. In case the objective of the problem is to minimize a function, the linear membership function presented in (15) would be employed.

$$\pi_i^r = \begin{cases} 1 & F_i^r \leq F_i^{min} \\ \dfrac{F_i^{max} - F_i^r}{F_i^{max} - F_i^{min}} & F_i^{min} \leq F_i^r \leq F_i^{max} \\ 0 & F_i^r \geq F_i^{max} \end{cases} \tag{15}$$

Note that the minimum and maximum values of each objective are denoted by F_i^{min} and F_i^{max}, respectively. Besides, the value of each objective within a Pareto optimal point and the associated membership function are described by F_i^r and π_i^r, respectively. It should be noted that this membership value specifies how much each Pareto optimal point is desired. Accordingly, a total membership value should be calculated for each member of the Pareto set. This total membership is obtained by using the relationship (16), where wf_i is the weighting factors allocated to the objective function and N represents the total number of objectives.

$$\pi^r = \frac{\sum_{i=1}^{N} wf_i \ \mu_i^r}{\sum_{i=1}^{N} wf_i} \tag{16}$$

IV. UNCERTAINTY HANDLING USING STOCHASTIC PROGRAMMING

This section describes the modeling of forecasting uncertainties in the microgrid. First, a large number of random scenarios is generated. Next, the number of scenarios is reduced to make the EED problem more tractable. Last, the deterministic DSD model (14) is transformed into a stochastic DSD model.

A. UNCERTAINTY MODELING

This paper considers the forecasting uncertainties related to the load demand, bid prices, wind turbine output, and photovoltaic output. The normal distribution is assumed to model the stochastic variations from the predicted values of load demand and bid prices. This paper assumes Beta distribution to model the stochastic variations of WT's and PV system's power outputs from their forecasted values, which is consistent with [41] and [44]. The two shape parameters α and β describe the Beta distribution. Let $P(t, DG)^{pred}$ be the predicted power with Beta distribution defined by α and β shape parameters. The variance and mean values are represented by $\sigma^2_{(t,DG)}$ and $\sigma_{(t,DG)}$, respectively. The $P(DG)^{cap}$ and S_{base} respectively define the size of the DG and power base for the system. The relationship of mean and variance values with shape parameters along with Beta function is given by [41] and [44]

$$f_{P(t,DG)^{pred}}(x) = x^{\alpha-1}(1-x)^{\beta-1} \tag{17a}$$

$$\frac{P(t,DG)^{pred}}{S_{base}} = \frac{\alpha_{(t,DG)}}{\alpha_{(t,DG)}+\beta_{(t,DG)}} \tag{17b}$$

$$\sigma^2_{(t,DG)} = \frac{\alpha_{(t,DG)}\,\beta_{(t,DG)}}{[\alpha_{(t,DG)}+\beta_{(t,DG)}]^2\,[\alpha_{(t,DG)}+\beta_{(t,DG)}+1]} \tag{17c}$$

$$\sigma_{(t,DG)} = 0.2 \times \frac{P(t,DG)^{pred}}{P(DG)^{cap}} + 0.21 \tag{17d}$$

Equations (17b)-(17c) at each time instant can be used to compute the shape parameters once the forecasted values are available for the wind and solar power generation. Note that there are two Beta functions for prediction errors in the scheduling problem. One Beta function is associated with the WT's power output while the other Beta function is associated with the photovoltaic system's power output. The normal distribution is employed to model the uncertainties of load demand and bid prices by assuming the forecasted values as mean values. The standard deviation in this paper is set to 4% of the forecasted values. It is pertinent to mention that the regression-based methods and machine learning techniques can predict the day-ahead load demand as well as the WT's and PV system's power output profiles but are beyond the scope of this paper.

The uncertainties in the forecasting are realized by producing a large number of random scenarios W. The computational burden is increased due to the large number of scenarios in a scenario-based optimization model. This situation essentially demands that the computational burden and solution accuracy should be traded-off. Here, a relatively good approximation of the original uncertainty is ensured by reducing the scenario number using simultaneous backward reduction method [38]. Let $\bar{s}$ denote the average value of scenarios and $||.||$ is the Euclidean norm. The distance function $d_{s,s'}$ for scenario pair (s, s') is given by

$$d_{s,s'} = \max\{1, ||s' - \bar{s}||, ||s - \bar{s}||\}\, ||s - s'|| \tag{18}$$

The aim is to compute w final scenarios after reducing the W initial scenarios. Reference [38] described in detail the steps involved in the simultaneous backward reduction method. This paper employs the GAMS/SCENRED2 tool [45] to obtain the final w reduced scenarios with associated aggregated probabilities denoted by ρ'_s. The GAMS/SCENRED2 tool ensures a reasonably good approximation of original uncertainty set by computing a scenario subset of the required cardinality or accuracy.

B. STOCHASTIC DSD MODEL

Different methods for uncertainty handling are proposed in multiobjective optimization problems (e.g., look at [46]). This section formulates a stochastic DSD model to compute the Pareto optimal solutions under forecasting uncertainties. The computational burden related to the stochastic optimization problem grows with any increase in the scenario number as it is a scenario-based optimization problem. Let $\mathbf{E}[Q]$ denote the expected value of an arbitrary objective function Q. The stochastic programming model in (19) is obtained by reformulating the deterministic DSD model in (14).

$$\begin{aligned} &\text{Minimize } \mathbf{E}[F_1 + F_2] \\ &\text{subject to (3), (5), (9)-(11).} \end{aligned} \tag{19}$$

Note that we calculate the expected value of the objective functions after determining the actual realization of forecasting uncertainties. The problem tractability is ensured by considering the finite number of reduced scenarios $\Omega_1, \ldots, \Omega_w$ with the associated probabilities of $\rho'_1, \ldots, \rho'_w$. The finite number of reduced scenarios enables the reformulation of the stochastic programming model in (19) by replacing the expectation term. The proposed stochastic DSD model at the kth utopia point is given by

$$\begin{aligned} &\text{Minimize } \sum_{s=1}^{w} \rho'_s[F_1 + F_2] \\ &\text{subject to (3), (5), (9)-(11).} \end{aligned} \tag{20}$$

The above model computes the optimal unit commitment and the related power dispatch while minimizing the total emissions and cost in the presence of forecasting uncertainties.

V. SIMULATION RESULTS AND ANALYSIS

The proposed DSD method is investigated by employing a low voltage (LV) microgrid test system ([18], [19]), a typical four-bus test network ([18], [39], [40], [47], [48]), and a large-scale IEEE 24-bus reliability test system (RTS) [49]. The effectiveness of the proposed method is established

TABLE 1. Thermal generating units' data for the four-bus network.

Plant	Unit	P_{MAX} (MW)	P_{MIN} (MW)	Greenhouse gas emission coefficients			Fuel cost coefficients		
				f_i (kg/h)	e_i (kg/MWh)	d_i (kg/MWh^2)	c_i ($/h)	b_i ($/MWh)	a_i ($/MWh^2)
1	G1	125.000	10.0000	13.8593	0.327670	0.00419000	756.799	38.5397	0.152740
	G2	150.000	10.0000	13.8593	0.327670	0.00419000	451.325	46.1592	0.105780
	G3	250.000	40.0000	40.2669	−0.545510	0.00683000	1049.32	40.3965	0.028030
2	G4	210.000	35.0000	40.2669	−0.545510	0.00683000	1243.53	38.3055	0.035460
	G5	325.000	130.000	42.8955	−0.511160	0.00461000	1658.57	36.3278	0.021110
3	G6	315.000	125.000	42.8955	−0.511160	0.00461000	1356.66	38.2704	0.017990

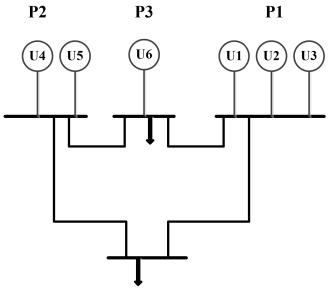

FIGURE 2. A typical four-bus test network.

by implementing several case studies involving deterministic and stochastic models. The MINLP problem is solved using GAMS [50] solvers on an ordinary desktop PC with 16.0 GB RAM and 3.30 GHz CPU. It is pertinent to mention here that the optimization problems are solved using the default settings of GAMS/SBB, GAMS/BONMIN, and GAMS/BARON solvers for making a fair comparison with the reported results in the literature.

A. DETERMINISTIC DSD MODEL FOR 4-BUS TEST SYSTEM

This subsection explores the deterministic directed search domain model for a typical 4-bus test network as shown in Fig. 2. The 4-bus system comprises of six thermal generating units and three plants. This case study considers the nitrogen oxides (NO_x) pollutant associated with the thermal generating units. This subsection aims to determine the optimal dispatch of thermal generating units while minimizing the emissions and cost. Here, a quadratic relationship is assumed between power generated by thermal generating units and cost/emission functions as expressed in (1b) and (2b). Table 1 depicts the power generation limits, greenhouse gas emission coefficients, and fuel cost coefficients of the six thermal generating units. The 4-bus test network has a total power demand of 900 MW.

It is important to estimate the power losses occurring in the transmission system. This case study formulates the transmission losses in the 4-bus test system using generating units' output power and B-loss coefficients as indicated in (4). The power balance is ensured by equating the total power generation in the network to the total power demand plus transmission losses. The B-loss coefficients for four-bus test network are illustrated in Table 2.

TABLE 2. B-loss coefficients for four-bus test network.

$$BL = \begin{bmatrix} 0.000091 & 0.000031 & 0.000029 \\ 0.000031 & 0.000062 & 0.000028 \\ 0.000029 & 0.000028 & 0.000072 \end{bmatrix}$$

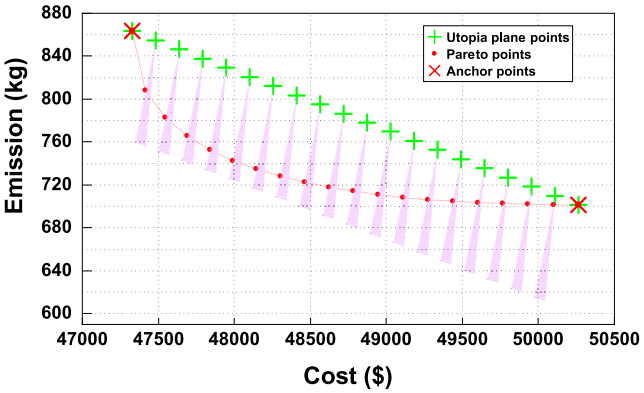

FIGURE 3. 4-bus test system: Transformed search cones using directed search domain method with angle $y_c = 10^o$.

This paper proposes the DSD algorithm to produce the well-distributed Pareto optimal set over a convex Pareto frontier. As described in Section III-A, the first step is the generation of two anchor points as depicted in Fig. 3. The ith row in the payoff table (ψ_1) illustrates an anchor point associated with the optimal value of the optimization problem with single objective function. It is apparent that the optimization problem with only fuel cost objective results in $ 47329.04 while the single-objective optimization with the emission objective function results in 701.46 kg emission. The next step is the generation of evenly distributed utopia plane points in accordance with (8). The deterministic DSD model generates a total of 20 utopia plane points while the optimization problem is solved for 18 times excluding the utopia points coinciding with the anchor points.

$$\psi_1 = \begin{pmatrix} 47329.04 & 863.28 \\ 50265.27 & 701.46 \end{pmatrix}$$

Fig. 3 indicates the quasi-evenly distributed set of Pareto points generated by the proposed DSD algorithm with an angle $y_c = 10^o$. It is evident from the convex Pareto frontier

TABLE 3. Comparison of simulation results with other algorithms reported in the literature.

Optimization method	[48]	[47]	[39]	[40]	[18]	Proposed DSD method
P1 (MW)	51.8200	51.8200	51.8200	51.8300	51.8200	46.267
P2 (MW)	32.660	32.6500	38.6400	38.6600	32.6500	32.864
P3 (MW)	209.790	208.780	248.730	248.740	208.770	157.23
P4 (MW)	128.120	128.120	122.140	122.150	128.120	156.401
P5 (MW)	291.950	292.020	252.020	252.030	292.030	272.022
P6 (MW)	223.570	223.570	223.570	223.580	223.570	273.667
Total cost ($/h)	47549.9	47549.0	47804.5	47809.0	47549.0	47425.163
Net emissions (kg/h)	823.360	823.350	843.420	843.530	823.350	805.743
Total losses (MW)	37.9100	36.9600	36.9200	36.9900	36.9600	38.452
Solution time (s)	12.0300	14.3600	0.195000	0.814000	12.5400	0.078

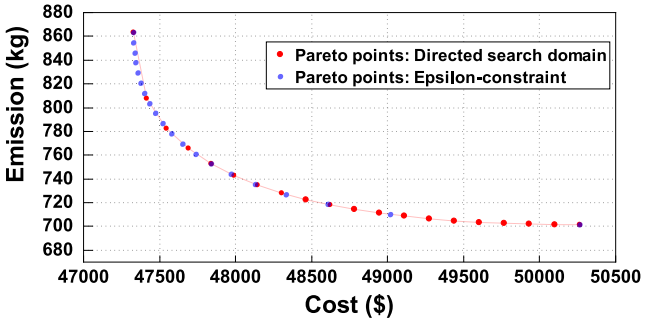

FIGURE 4. 4-bus test system: Pareto optimal solutions with angle $\gamma_c = 10^o$ [Directed search domain vs Epsilon-constraint method].

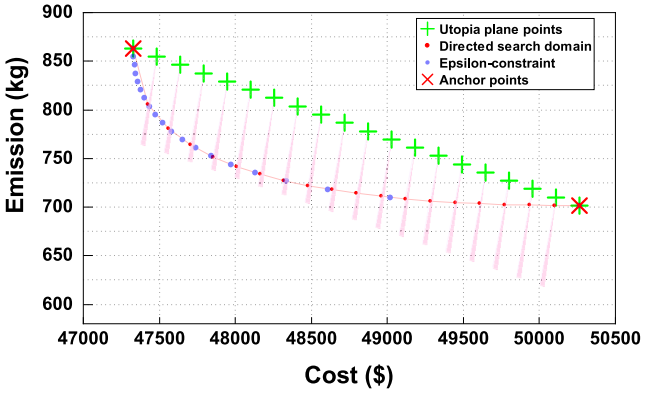

FIGURE 5. 4-bus test system: Transformed search cones using DSD method with angle $\gamma_c = 5^o$.

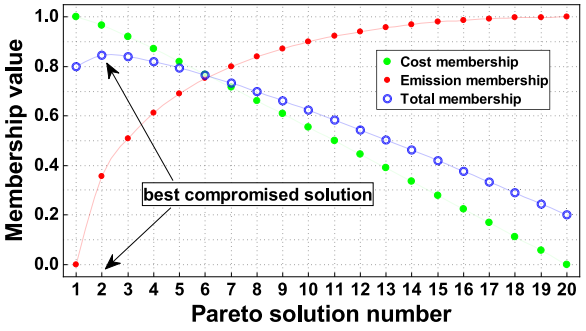

FIGURE 6. 4-bus test system: Variation of membership values versus Pareto points with same weighting factors for $\gamma_c = 5^o$.

that both objective functions are of competing nature. The shaded portions depict the transformed search cones after shrinking the original search domain. Note that the search domain is shrunk by the transform like a ''light beam'' emitting out of the utopia plane point and highlighting a spot (i.e., Pareto optimal solution) on Pareto frontier. The small angle $\gamma_c = 10^o$ leads to quasi-evenly distributed Pareto optimal points by limiting the search space and avoiding the generation of redundant solutions for different optimization runs. The average computation time for a single Pareto point is 0.0459 s while the total computation time to obtain the 18 Pareto optimal points is 0.827 s using GAMS/SBB.

Figs. 4 and 5 compare the distribution of Pareto points generated by DSD method with that of epsilon-constraint method as described in [51]. The Pareto points obtained by epsilon-constraint method are mostly concentrated in the upper-left portion of Pareto frontier. By contrast, the DSD method results in the Pareto points with the quasi-even distribution on the entire Pareto frontier. This quasi-evenly distributed set of Pareto points is of paramount importance as it aids the system operator to make a well-informed decision by analyzing only a very limited number of the Pareto optimal points.

Fig. 6 illustrates the best desired solution computed by the Fuzzy decision maker. The objective functions are assigned the same weighting factors before the computation of total membership, emission membership, and cost membership values. The best trade-off Pareto point is the Pareto solution number 2 as its total membership value of 0.845 is the maximum. Table 3 compares the simulation results of the presented DSD algorithm with the other algorithms reported in the literature. The proposed DSD method results in fuel cost of $ 47425.163 while the emission obtained are lowest as compared to the other approaches described in the literature. These empirical results establish the effectiveness of the proposed DSD method for environmental/economic scheduling of a microgrid.

B. DETERMINISTIC DSD MODEL FOR LV MICROGRID WITHOUT DETAILED BATTERY STORAGE MODELING

This subsection explores the deterministic DSD method for a typical low voltage microgrid test system as illustrated in

TABLE 4. Data of the DG sources and utility for LV microgrid model [19].

Type	NO_x (kg/MWh)	SO_2 (kg/MWh)	CO_2 (kg/MWh)	SUC/SDC (€ct)	Bid (€ct/kWh)	P_{MAX} (kW)	P_{MIN} (kW)
MT	0.1000	0.003600	720.0	0.9600	0.4570	30.00	6.000
FC	0.007500	0.003000	460.0	1.650	0.2940	30.00	3.000
PV	0.000	0.000	0.000	0.000	2.5840	25.00	0.000
WT	0.000	0.000	0.000	0.000	1.0730	15.00	0.000
Bat	0.001000	0.0002000	10.00	0.000	0.3800	30.00	−30.00
Utility	0.000	0.000	0.000	0.000	Table 5	30.00	−30.00

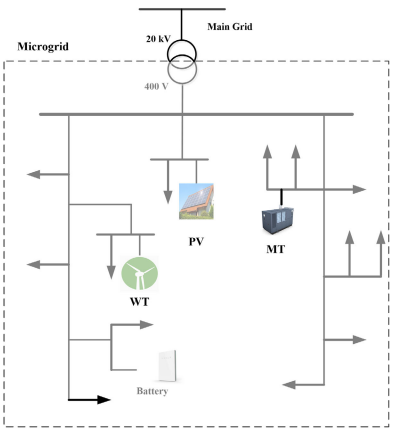

FIGURE 7. A typical low voltage microgrid test system.

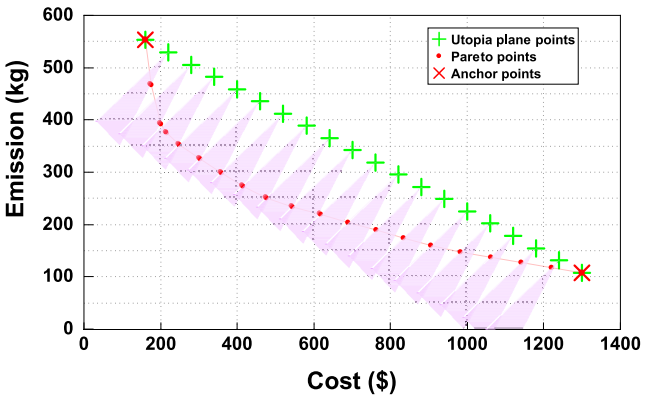

FIGURE 8. LV microgrid test system: Transformed search cones using the DSD method with angle $\gamma_c = 10^o$.

Fig. 7. This LV microgrid model includes MTs, FCs, PV system, WTs, and BA. This case study considers the CO_2, NO_x, and SO_2 pollutants. The objective is to minimize the total greenhouse gas emissions and cost. The total cost comprises of the shut-down/start-up costs and power generation costs of distributed generators. The power sources are dispatched on hourly basis and the total scheduling time horizon is 24 hours. It is assumed that there is no reactive power contribution from distributed generators as these are operated at unity power factor. The LV microgrid connects with the utility through a power exchange link. The MGCC incorporates the optimization algorithm to compute the optimal unit commitment and associated dispatch for the efficient operation of microgrid.

Table 4 summarizes the existing data of the distributed generators and utility for LV microgrid test system as tabulated in [19]. The emissions assumed by DG sources are in kilogram per MWh while cents of Euro per kWh (€ct/kWh) are used for bid coefficients. The energy capacity of the battery storage is assumed to be 1 MWh and charging/discharging efficiencies are set to 100%. The initial state-of-charge is assumed to be 100%. This assumption enables the battery storage to discharge during the scheduling period without worrying about the charging operation. Next subsection includes the detailed battery storage model. Any other parameter settings can be assumed depending on the data of the system under consideration. It is apparent that the utility, WT, and PV system are considered emission-free in this deterministic DSD model. The forecasted output of the PV system, WT, electrical energy price, and load demand are illustrated in Table 5. The energy price and load demand profiles are adopted from [18] and [19] while the WT and PV system's output profiles from [51] are considered.

Fig. 8 indicates the well-distributed Pareto optimal points over convex Pareto frontier computed by the proposed DSD algorithm with an angle $\gamma_c = 10^o$. The ith row in the payoff table (ψ_2) corresponds to the minimization of one and only one objective within the objective space. The small angle $\gamma_c = 10^o$ helps to avoid the generation of redundant solutions for different optimization runs. The total solution time to compute 18 Pareto optimal points is 243 s using GAMS/SBB while the average CPU time for the computation of single Pareto point is 13.5 s.

$$\psi_2 = \begin{pmatrix} 160.77 & 552.67 \\ 1299.49 & 108.11 \end{pmatrix}$$

Figs. 9 and 10 compare the distribution of Pareto optimal points generated by the DSD algorithm with that of epsilon-constraint method [51]. Note that the epsilon-constraint method here uses payoff table (ψ_2) for making a fair comparison. The quasi-even distribution of Pareto solutions on the Pareto frontier as compared to the epsilon-constraint technique is apparent from Figs. 9 and 10. It can be observed that the transformed search cones help to explore the Pareto frontier in a controlled manner according to the system operator's needs. The first two Pareto optimal solutions (from the left side in Fig. 10) computed by the DSD method are located at the lower edges of the search cones while the remaining Pareto points are located at the upper edges of the search cones. This is somewhat different

TABLE 5. Forecasted output of wind turbine, photovoltaic system, load demand, and bids ([18], [19], [51]).

Hour	Electrical energy price (€ct/kWh)	Load (kW)	Forecasted output (kW)	
			WT	PV
1	0.2300	52.00	1.785	0.000
2	0.1900	50.00	1.785	0.000
3	0.1400	50.00	1.785	0.000
4	0.1200	51.00	1.785	0.000
5	0.1200	56.00	1.785	0.000
6	0.2000	63.00	0.9140	0.000
7	0.2300	70.00	1.785	0.000
8	0.3800	75.00	1.308	0.1940
9	2.500	76.00	1.785	3.754
10	4.000	80.00	3.085	7.528
11	4.000	78.00	8.772	10.44
12	4.000	74.00	10.413	11.96
13	1.500	72.00	3.923	23.89
14	4.000	72.00	2.377	21.05
15	2.000	76.00	1.785	7.865
16	1.950	80.00	1.302	4.221
17	0.6000	85.00	1.785	0.5390
18	0.4100	88.00	1.785	0.000
19	0.3500	90.00	1.302	0.000
20	0.4300	87.00	1.785	0.000
21	1.170	78.00	1.302	0.000
22	0.5400	71.00	1.302	0.000
23	0.3000	65.00	0.9140	0.000
24	0.2600	56.00	0.6120	0.000

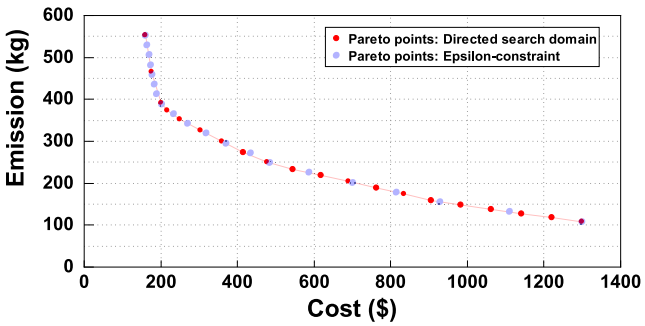

FIGURE 9. LV microgrid test system: Pareto optimal solutions with angle $\gamma_c = 10^o$ [Directed search domain vs epsilon-constraint method].

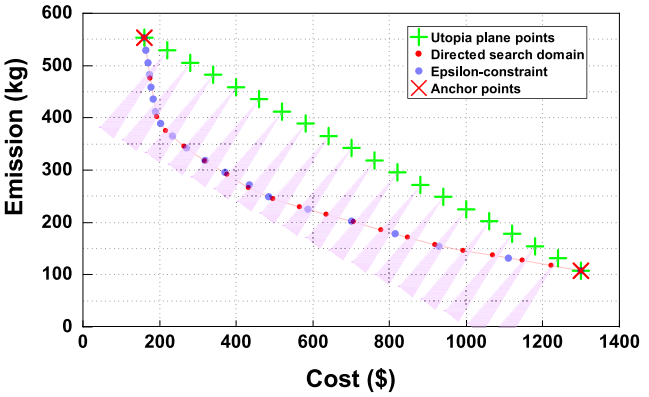

FIGURE 10. LV microgrid test system: Transformed search cones using the DSD method with angle $\gamma_c = 5^o$.

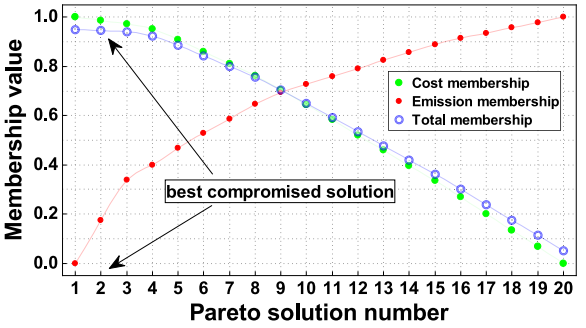

FIGURE 11. LV microgrid test system: Variation of membership values versus Pareto points with same weighting factors for $\gamma_c = 5^o$.

from Fig. 8 where the Pareto optimal point (215.60, 374.62) is located inside the transformed search cone instead of its edges.

Fig. 11 illustrates the most desired solution obtained by employing the Fuzzy decision maker [52]. The Pareto points with fair emissions and cost are assumed to be computed by the system operator, so each objective function is set with same weighting factors. The best trade-off Pareto point is the Pareto solution number 2 as its total membership value of 0.947 is maximum. The emission membership value for the Pareto solution number 2 is 0.175 while the cost membership value is 0.987. Table 6 reports the results computed by the proposed DSD algorithm for LV microgrid test network. The proposed DSD method results in the total cost of 175.005 €ct and greenhouse gas emission of 474.812 kg. It is apparent from Table 6 that Pareto solution number 2 is a feasible solution. Moreover, the load demand is majorly supplied by the utility grid from hours 1 to 8 via a point of common coupling as utility bid prices are relatively low compared to bids of other units. Note that the renewable energy sources such as wind turbines and photovoltaic systems lead to the reduction of pollutants as their emission coefficients are zero.

C. DETERMINISTIC DSD MODEL FOR LV MICROGRID WITH DETAILED BATTERY STORAGE MODELING

This case study aims to demonstrate the full satisfaction of battery storage constraints. The detailed battery storage model (6) governs the charging and discharging operation of the battery in LV microgrid test system as depicted in Fig. 7. Table 4 illustrates the data of the DG sources and utility for LV microgrid. The energy capacity of the battery storage is assumed to be 1 MWh and charging/discharging efficiencies are set to 100%. The initial state-of-charge is assumed to be 20% in (6d). The battery storage is allowed to operate between 0% and 100% of its rated capacity as per (6b). Any other parameter settings can be considered depending on the operational requirements.

The objective is to minimize the total greenhouse gas emissions and cost while satisfying the battery storage constraints. Fig. 12 shows the quasi-even distribution of Pareto optimal points over the Pareto frontier computed by the proposed

TABLE 6. Results computed by the proposed DSD algorithm for LV microgrid test network.

Hour	Proposed DSD method [Power dispatch (kW)]					
	MT	FC	PV	WT	Battery	Utility
1	0	0	0	0	22	30
2	0	0	0	0	20	30
3	0	0	0	0	20	30
4	0	0	0	0	21	30
5	0	0	0	0	26	30
6	0	28.447	0	0	4.553	30
7	0	27.782	0	0	12.218	30
8	0	27.76	0	0	17.24	30
9	30	30	0	1.786	30	−15.785
10	30	30	7.528	3.085	30	−20.613
11	30	30	9.228	8.772	30	−30
12	30	30	0	10.413	30	−26.413
13	30	30	0	3.923	30	−21.923
14	30	30	0	2.377	30	−20.377
15	30	30	0	1.786	30	−15.786
16	30	30	0	1.302	30	−11.302
17	30	30	0	0	30	−5
18	0	30	0	0	30	28
19	0	30	0	0	30	30
20	0	30	0	0	30	27
21	30	30	0	1.302	30	−13.302
22	0	30	0	0	30	11
23	0	20	0	0	15	30
24	0	26	0	0	0	30
	Total cost (€ct)		**175.0**	**Total emissions (kg)**		474.8

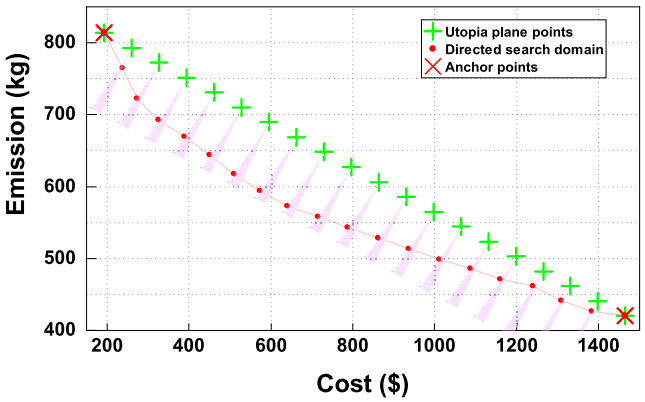

FIGURE 12. LV microgrid test system: Transformed search cones using the DSD method with an angle $\gamma_c = 5^o$.

DSD method using the payoff table (ψ_3).

$$\psi_3 = \begin{pmatrix} 193.284 & 813.677 \\ 1465.347 & 419.886 \end{pmatrix}$$

Fig. 13(a) describes the charging and discharging operation of the battery storage corresponding to the best trade-off Pareto solution number 9 as computed by the Fuzzy decision maker. The battery storage is mainly charging between 01:00 and 05:00 when the utility bid prices are relatively low as illustrated in Table 5. By contrast, the battery storage is mostly discharging between 10:00 and 12:00 to partially supply the load demand when utility bid prices are relatively high. Note that the battery storage active power flow is fully satisfying the constraints (6e)-(6f) as it remains between −30 kW and 30 kW. Also, Fig. 13(b) shows the full satisfaction of constraint (6d) as the final state-of-charge of 20%

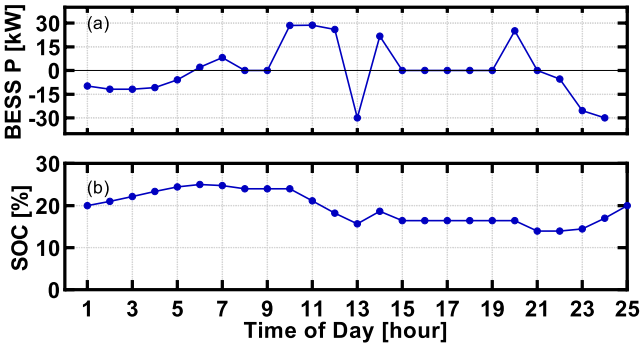

FIGURE 13. LV microgrid test system: (a) Battery storage active power flow. (b) Battery storage state-of-charge.

is the same as the initial state-of-charge. The battery storage in Fig. 13(a) charges between 22:00-24:00 to meet the constraint (6d) as the utility bid prices are relatively low at these time instants. The renewable energy sources such as wind turbines and photovoltaic systems play their role towards the minimization of overall pollutant emissions.

D. DETERMINISTIC DSD MODEL FOR IEEE RTS 24-BUS SYSTEM

This subsection demonstrates the scalability of the proposed DSD method for the EED problem by considering an updated version of large-scale IEEE RTS 24-bus system [49] that was originally introduced in [53]. The objective is to reduce the total greenhouse gas emissions and costs. The single line diagram and associated constraints of IEEE RTS 24-bus system are not included here for brevity purposes. The interested readers are referred to [54] for the detailed modeling of IEEE RTS 24-bus system. The greenhouse gas emission coefficients are assumed to be the same as in [55]. The IEEE RTS 24-bus system consists of 34 transmission lines and 17 loads. The units are dispatched on an hourly basis with the 24 hours scheduling time horizon.

Fig. 14 compares the distribution of Pareto optimal points generated by the DSD method with that of epsilon-constraint technique. Note that both methods use the payoff table (ψ_4) for making a fair comparison. The DSD method results in the quasi-even distribution of Pareto optimal points on the Pareto frontier as compared to the epsilon-constraint method as evident from Fig. 14. The Pareto points computed by the epsilon-constraint technique are mostly located in the upper-left region of the Pareto frontier. This attribute indicates the effectiveness of the proposed DSD method in finding the evenly distributed Pareto set; thus, enabling the system operator to analyze the whole Pareto frontier with a very limited number of Pareto optimal points.

$$\psi_4 = \begin{pmatrix} 522870.34 & 112721.16 \\ 480793.85 & 158584.27 \end{pmatrix}$$

Fig. 15 describes the best desired solution computed by the Fuzzy decision maker with the same weighting factors. The best trade-off point is the Pareto solution number 12 as

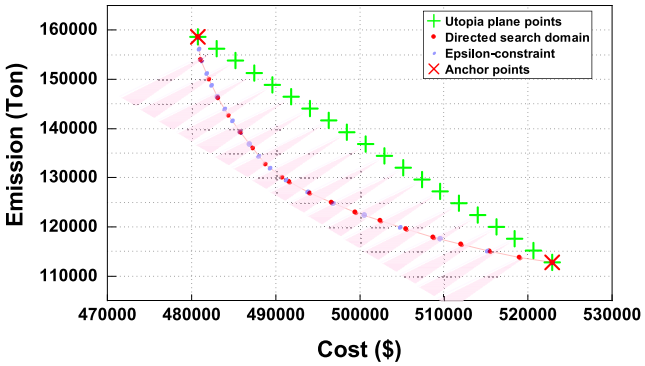

FIGURE 14. IEEE RTS 24-bus system: Transformed search cones using the DSD method with an angle $\gamma_c = 5^o$.

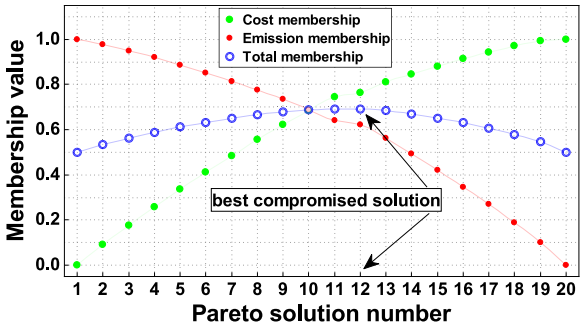

FIGURE 15. IEEE RTS 24-bus system: Variation of membership values versus Pareto points with same weighting factors for $\gamma_c = 5^o$.

its total membership value of 0.693 is the maximum. The cost membership value for the Pareto solution number 12 is 0.763 while the emission membership value is 0.622. The total solution time to compute 18 Pareto optimal points is 9.985 s using GAMS/BONMIN solver.

E. STOCHASTIC DSD MODEL FOR LV MICROGRID TEST SYSTEM

This subsection explores the stochastic DSD model for a typical low voltage microgrid test system as depicted in Fig. 7. The unit data and forecasted output related to LV microgrid test system are illustrated in Tables 4 and 5. Here, the case study considers the forecasting uncertainties associated with the load demand, PV system's output, WT's output, and bid prices. The normal distribution is assumed to model the stochastic variations from the forecasted values of load demand and bid prices. Also, the Beta distribution is employed to model the stochastic variations of PV system's and WT's outputs from their predicted values. This subsection generates a total of 500 initial scenarios to model the forecasting uncertainties. The stochastic programming is implemented after reducing the scenario number to 20 using the simultaneous backward reduction method as detailed in Section IV-A. The original system uncertainty with a relatively good approximation is ensured while the computational burden is minimized by lowering the number of scenarios. The objective is to compute the optimal unit commitment

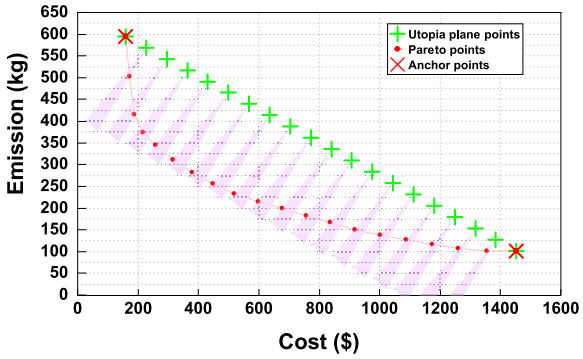

FIGURE 16. LV microgrid test system: Transformed search cones using the DSD method with an angle $\gamma_c = 5^o$ and *scenarios* = 20.

and the related power dispatch while minimizing the total emissions and cost. The total scheduling time is 24 hours while the units are dispatched on an hourly basis.

Fig. 16 depicts the Pareto set that is well-distributed over the convex Pareto frontier using the proposed stochastic DSD model with an angle $\gamma_c = 5^o$. The convex nature of Pareto frontier is attributed to the conflicting nature of objectives. The linear combination of total emission and cost functions forms the aggregate objective function. It is apparent from the payoff table (ψ_5) that the cost as the only objective function is 158.99 €ct while emission as the only objective function is 101.47 kg. Equation (8) uses the anchor points in the payoff table to generate the utopia plane points. The evenly distributed utopia plane points result in the quasi-even distribution of Pareto solutions as can be observed in Fig. 16. The stochastic DSD model generates 20 utopia plane points while the stochastic problem is solved for 18 times excluding the anchor points. It is pertinent to mention that the proposed DSD algorithm is the ideal candidate of parallel processing as separate Pareto search can be conducted for each utopia plane point. The parallel processing along with the choice of reduced scenario number and total Pareto points can decrease the computational burden significantly.

$$\psi_5 = \begin{pmatrix} 158.99 & 595.29 \\ 1452.80 & 101.47 \end{pmatrix}$$

It can be observed that the first two stochastic Pareto points (from the left side in Fig. 16) computed by the proposed method are located at the lower edges of the search cones. The remaining stochastic Pareto optimal points are located at the upper edges of the search cones with the exemption of Pareto point (215.92, 374.69) that lies inside the search cone. This is somewhat different from the deterministic DSD model with an angle $\gamma_c = 5^o$ in Fig. 10 where all the Pareto solutions lie on the edges of the search cones. Fig. 17 shows the best trade-off solution computed by employing the Fuzzy decision maker. The same weighting factors are assumed to determine the Pareto points with fair emission and cost. The quasi-evenly distributed set of Pareto points provides the significant information about the Pareto frontier to the system operator with a minimum computational burden. The most

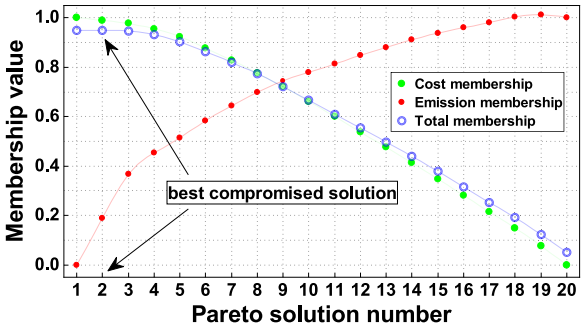

FIGURE 17. LV microgrid test system: Variation of membership values versus Pareto points with same weighting factors for $\gamma_c = 5^o$ and *scenarios* = 20.

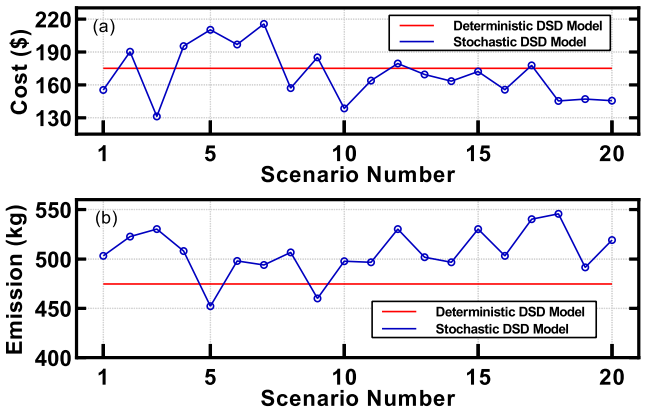

FIGURE 18. LV microgrid test system: (a) Operating cost objective. (b) Pollutant emission objective.

desired Pareto point is the Pareto solution number 2 as its total membership value of 0.950 is maximum.

Fig. 18 compares the objective values computed by the deterministic DSD model with that of stochastic DSD model for Pareto solution number 2. The proposed stochastic (deterministic) DSD model results in a total cost of 171.701 €ct (175.005 €ct) and greenhouse gas emissions of 503.292 kg (474.812 kg). Note that the aggregate objective function AOF = 649.818 using deterministic DSD model (14) while the stochastic DSD model (20) results in AOF = 674.993 for 20 scenarios. It is apparent that the forecasting uncertainties result in higher aggregate objective function value for Pareto solution number 2. The deterministic and stochastic case studies in this paper establish the effectiveness of the proposed DSD models for the environmental/economic scheduling of a microgrid.

VI. CONCLUSION

This paper presented a directed search domain algorithm to solve the day-ahead environmental/economic scheduling problem of a renewable energy based microgrid. The DSD algorithm performed the shrinking of the original search domains into hypercones. This shrinking helped to avoid the generation of redundant solutions and resulted in an evenly-distributed Pareto points with the minimum computational burden. This paper computed the optimal unit commitment and the related power dispatch while simultaneously reducing the total operating cost and pollutant emissions. The microgrid assets included MTs, FCs, PV systems, battery storage, and WTs. Unlike other works, this research work employed stochastic programming to account for the forecasting uncertainties related to load demand, prices, wind, and photovoltaic outputs. By reducing the number of scenarios, computational complexity was traded-off for the solution accuracy. The best trade-off solution among all the Pareto optimal points can be determined by employing the Fuzzy satisfying technique. The proposed DSD method with a total cost $ 47425.163 and net emissions 805.743 kg outperformed the analytical strategy based on a single equivalent objective function with total cost $ 47804.5 and net emissions 843.42 kg. Also, the proposed DSD method resulted in quasi-evenly distributed Pareto optimal points as opposed to the epsilon-constraint method for 4-bus test system, LV microgrid test system, and IEEE RTS 24-bus system. The empirical results demonstrated the potential of the proposed deterministic and stochastic DSD models in terms of computational time, objective values, and quasi-even distribution of Pareto optimal points.

REFERENCES

[1] G. Pepermans, J. Driesen, D. Haeseldonckx, R. Belmans, and W. D'haeseleer, "Distributed generation: Definition, benefits and issues," *Energy Policy*, vol. 33, no. 6, pp. 787–798, Apr. 2005.

[2] J. M. Guerrero, F. Blaabjerg, T. Zhelev, K. Hemmes, E. Monmasson, S. Jemei, M. P. Comech, R. Granadino, and J. I. Frau, "Distributed generation: Toward a new energy paradigm," *IEEE Ind. Electron. Mag.*, vol. 4, no. 1, pp. 52–64, Mar. 2010.

[3] M. Edmonds and T. Miller, "The next 50 years: What's next for the grid?" *IEEE Power Energy Mag.*, vol. 12, no. 2, pp. 92–96, Mar. 2014.

[4] P. Cortés, P. Auladell-León, J. Muñuzuri, and L. Onieva, "Near-optimal operation of the distributed energy resources in a smart microgrid district," *J. Cleaner Prod.*, vol. 252, Apr. 2020, Art. no. 119772.

[5] J. Huang, C. Jiang, and R. Xu, "A review on distributed energy resources and MicroGrid," *Renew. Sustain. Energy Rev.*, vol. 12, no. 9, pp. 2472–2483, 2008.

[6] M. H. Bellido, L. P. Rosa, A. O. Pereira, D. M. Falcão, and S. K. Ribeiro, "Barriers, challenges and opportunities for microgrid implementation: The case of federal university of Rio de Janeiro," *J. Cleaner Prod.*, vol. 188, pp. 203–216, Jul. 2018.

[7] M. A. S. Hassan, M. Chen, H. Lin, M. H. Ahmed, M. Z. Khan, and G. R. Chughtai, "Optimization modeling for dynamic price based demand response in microgrids," *J. Cleaner Prod.*, vol. 222, pp. 231–241, Jun. 2019.

[8] M. Ross, C. Abbey, F. Bouffard, and G. Joós, "Microgrid economic dispatch with energy storage systems," *IEEE Trans. Smart Grid*, vol. 9, no. 4, pp. 3039–3047, Jul. 2018.

[9] M. A. Velasquez, J. Barreiro-Gomez, N. Quijano, A. I. Cadena, and M. Shahidehpour, "Intra-hour microgrid economic dispatch based on model predictive control," *IEEE Trans. Smart Grid*, vol. 11, no. 3, pp. 1968–1979, May 2020.

[10] G. Chen and Z. Zhao, "Delay effects on consensus-based distributed economic dispatch algorithm in microgrid," *IEEE Trans. Power Syst.*, vol. 33, no. 1, pp. 602–612, Jan. 2018.

[11] M. Yu, C. Song, S. Feng, and W. Tan, "A consensus approach for economic dispatch problem in a microgrid with random delay effects," *Int. J. Electr. Power Energy Syst.*, vol. 118, Jun. 2020, Art. no. 105794.

[12] W. Chen, Z. Shao, K. Wakil, N. Aljojo, S. Samad, and A. Rezvani, "An efficient day-ahead cost-based generation scheduling of a multi-supply microgrid using a modified krill herd algorithm," *J. Cleaner Prod.*, vol. 272, Nov. 2020, Art. no. 122364.

[13] P. Aliasghari, B. Mohammadi-Ivatloo, M. Alipour, M. Abapour, and K. Zare, "Optimal scheduling of plug-in electric vehicles and renewable micro-grid in energy and reserve markets considering demand response program," *J. Cleaner Prod.*, vol. 186, pp. 293–303, Jun. 2018.
[14] J. H. Talaq, F. El-Hawary, and M. E. El-Hawary, "A summary of environmental/economic dispatch algorithms," *IEEE Trans. Power Syst.*, vol. 9, no. 3, pp. 1508–1516, Aug. 1994.
[15] IEA. (2021). *Net Zero by 2050, International Energy Agency (IEA)*. Paris. [Online]. Available: https://www.iea.org/reports/net-zero-by-2050
[16] T. Erfani and S. V. Utyuzhnikov, "Directed search domain: A method for even generation of the Pareto frontier in multiobjective optimization," *Eng. Optim.*, vol. 43, no. 5, pp. 467–484, May 2011.
[17] S. V. Utyuzhnikov, P. Fantini, and M. D. Guenov, "A method for generating a well-distributed Pareto set in nonlinear multiobjective optimization," *J. Comput. Appl. Math.*, vol. 223, no. 2, pp. 820–841, Jan. 2009.
[18] A. A. Moghaddam, A. Seifi, T. Niknam, and M. R. A. Pahlavani, "Multi-objective operation management of a renewable MG (micro-grid) with back-up micro-turbine/fuel cell/battery hybrid power source," *Energy*, vol. 36, no. 11, pp. 6490–6507, Nov. 2011.
[19] A. A. Moghaddam, A. Seifi, and T. Niknam, "Multi-operation management of a typical micro-grids using particle swarm optimization: A comparative study," *Renew. Sustain. Energy Rev.*, vol. 16, no. 2, pp. 1268–1281, 2012.
[20] T. C. Bora, V. C. Mariani, and L. D. S. Coelho, "Multi-objective optimization of the environmental-economic dispatch with reinforcement learning based on non-dominated sorting genetic algorithm," *Appl. Thermal Eng.*, vol. 146, pp. 688–700, Jan. 2019.
[21] Z. Xin-gang, L. Ji, M. Jin, and Z. Ying, "An improved quantum particle swarm optimization algorithm for environmental economic dispatch," *Exp. Syst. Appl.*, vol. 152, Aug. 2020, Art. no. 113370.
[22] M. Roslan, M. Hannan, P. J. Ker, R. Begum, T. I. Mahlia, and Z. Dong, "Scheduling controller for microgrids energy management system using optimization algorithm in achieving cost saving and emission reduction," *Appl. Energy*, vol. 292, Jun. 2021, Art. no. 116883.
[23] Y.-H. Bui, A. Hussain, and H.-M. Kim, "Double deep *Q*-learning-based distributed operation of battery energy storage system considering uncertainties," *IEEE Trans. Smart Grid*, vol. 11, no. 1, pp. 457–469, Jan. 2020.
[24] J. Jithendranath and D. Das, "Scenario-based multi-objective optimisation with loadability in islanded microgrids considering load and renewable generation uncertainties," *IET Renew. Power Gener.*, vol. 13, no. 15, pp. 785–800, Apr. 2019.
[25] M. Ghiasi, T. Niknam, M. Dehghani, P. Siano, H. H. Alhelou, and A. Al-Hinai, "Optimal multi-operation energy management in smart microgrids in the presence of RESs based on multi-objective improved DE algorithm: Cost-emission based optimization," *Appl. Sci.*, vol. 11, no. 8, p. 3661, Apr. 2021.
[26] B. Dey, B. Bhattacharyya, and F. P. G. Márquez, "A hybrid optimization-based approach to solve environment constrained economic dispatch problem on microgrid system," *J. Cleaner Prod.*, vol. 307, Jul. 2021, Art. no. 127196.
[27] L. Bayon, J. M. Grau, M. M. Ruiz, and P. M. Suarez, "The exact solution of the environmental/economic dispatch problem," *IEEE Trans. Power Syst.*, vol. 27, no. 2, pp. 723–731, May 2012.
[28] W. Wei, J. Wang, and S. Mei, "Convexification of the Nash bargaining based environmental-economic dispatch," *IEEE Trans. Power Syst.*, vol. 31, no. 6, pp. 5208–5209, Nov. 2016.
[29] A. M. Jubril and A. O. Adediji, "Semi-definite programming approach to stochastic combined heat and power environmental/economic dispatch problem," *Electric Power Compon. Syst.*, vol. 43, no. 18, pp. 2039–2049, Sep. 2015.
[30] M. Narimani, Maigha, J.-Y. Joo, and M. Crow, "Multi-objective dynamic economic dispatch with demand side management of residential loads and electric vehicles," *Energies*, vol. 10, no. 5, p. 624, May 2017.
[31] A. Ahmadi, A. Kaymanesh, P. Siano, M. Janghorbani, A. E. Nezhad, and D. Sarno, "Evaluating the effectiveness of normal boundary intersection method for short-term environmental/economic hydrothermal self-scheduling," *Electric Power Syst. Res.*, vol. 123, pp. 192–204, Jun. 2015.
[32] T. Erfani, S. V. Utyuzhnikov, and B. Kolo, "A modified directed search domain algorithm for multiobjective engineering and design optimization," *Struct. Multidisciplinary Optim.*, vol. 48, no. 6, pp. 1129–1141, Dec. 2013.
[33] A. Ahmadi, M. R. Ahmadi, and A. E. Nezhad, "A lexicographic optimization and augmented ϵ-constraint technique for short-term environmental/economic combined heat and power scheduling," *Electr. Power Compon. Syst.*, vol. 42, no. 9, pp. 945–958, May 2014.
[34] M. Saffari, M. Kia, V. Vahidinasab, and K. Mehran, "Integrated active/reactive power scheduling of interdependent microgrid and EV fleets based on stochastic multi-objective normalised normal constraint," *IET Gener., Transmiss. Distrib.*, vol. 14, no. 11, pp. 2055–2064, Jun. 2020.
[35] S. Utyuzhnikov, P. Fantini, and M. Guenov, "Numerical method for generating the entire Pareto frontier in multiobjective optimization," in *Proc. Eurogen*, 2005, pp. 12–14.
[36] S. Rahmani and N. Amjady, "Optimal operation strategy for multi-carrier energy systems including various energy converters by multi-objective information gap decision theory and enhanced directed search domain method," *Energy Convers. Manage.*, vol. 198, Oct. 2019, Art. no. 111804.
[37] S. Rahmani and N. Amjady, "Non-deterministic optimal power flow considering the uncertainties of wind power and load demand by multi-objective information gap decision theory and directed search domain method," *IET Renew. Power Gener.*, vol. 12, pp. 1354–1365, Sep. 2018.
[38] L. Wu, M. Shahidehpour, and T. Li, "Stochastic security-constrained unit commitment," *IEEE Trans. Power Syst.*, vol. 22, no. 2, pp. 800–811, May 2007.
[39] C. Palanichamy and N. Babu, "Analytical solution for combined economic and emissions dispatch," *Elect. Power Syst. Res.*, vol. 78, no. 7, pp. 1129–1139, 2008.
[40] C. Palanichamy and K. Srikrishna, "Economic thermal power dispatch with emission constraint," *J. Indian Inst. Eng.*, vol. 72, no. 11, pp. 6490–6507, 1991.
[41] R. Zafar, J. Ravishankar, J. E. Fletcher, and H. R. Pota, "Multi-timescale model predictive control of battery energy storage system using conic relaxation in smart distribution grids," *IEEE Trans. Power Syst.*, vol. 33, no. 6, pp. 7152–7161, Nov. 2018.
[42] B. Xin, L. Chen, J. Chen, H. Ishibuchi, K. Hirota, and B. Liu, "Interactive multiobjective optimization: A review of the state-of-the-art," *IEEE Access*, vol. 6, pp. 41256–41279, 2018.
[43] A. E. Nezhad, M. S. Javadi, and E. Rahimi, "Applying augmented ϵ-constraint approach and lexicographic optimization to solve multi-objective hydrothermal generation scheduling considering the impacts of pumped-storage units," *Int. J. Electr. Power Energy Syst.*, vol. 55, pp. 195–204, Feb. 2014.
[44] Z. Wang, J. Wang, B. Chen, M. M. Begovic, and Y. He, "MPC-based voltage/var optimization for distribution circuits with distributed generators and exponential load models," *IEEE Trans. Smart Grid*, vol. 5, no. 5, pp. 2412–2420, Sep. 2014.
[45] (2008). *GAMS/SCENRED2 Documentation*. [Online]. Available: https://www.gams.com/24.8/docs/tools/scenred2/index.html
[46] T. Erfani and S. V. Utyuzhnikov, "Control of robust design in multi-objective optimization under uncertainties," *Structural Multidisciplinary Optim.*, vol. 45, no. 2, pp. 247–256, Feb. 2012.
[47] M. Motevasel and A. R. Seifi, "Expert energy management of a micro-grid considering wind energy uncertainty," *Energy Convers. Manage.*, vol. 83, pp. 58–72, Jul. 2014.
[48] J. Cai, X. Ma, Q. Li, L. Li, and H. Peng, "A multi-objective chaotic particle swarm optimization for environmental/economic dispatch," *Energy Convers. Manage.*, vol. 50, no. 5, pp. 1318–1325, 2009.
[49] C. Ordoudis, P. Pinson, J. M. M. González, and M. Zugno, "An updated version of the IEEE RTS 24-bus system for electricity market and power system operation studies," Dept. Elect. Eng., Dept. Appl. Math. Comput. Sci., Tech. Univ. Denmark, Lyngby, Denmark, Tech. Rep., 2016.
[50] A. Brooke, D. Kendrick, and A. Meeraus, *GAMS User's Guide*. Singapore: Scientific Press, 2012.
[51] A. Rezvani, M. Gandomkar, M. Izadbakhsh, and A. Ahmadi, "Environmental/economic scheduling of a micro-grid with renewable energy resources," *J. Cleaner Prod.*, vol. 87, pp. 216–226, Jan. 2015.
[52] M. R. Norouzi, A. Ahmadi, A. E. Nezhad, and A. Ghaedi, "Mixed integer programming of multi-objective security-constrained hydro/thermal unit commitment," *Renew. Sustain. Energy Rev.*, vol. 29, pp. 911–923, Jan. 2014.
[53] C. Grigg, P. Wong, P. Albrecht, R. Allan, M. Bhavaraju, R. Billinton, Q. Chen, C. Fong, S. Haddad, S. Kuruganty, and W. Li, "The IEEE reliability test system-1996. A report prepared by the reliability test system task force of the application of probability methods subcommittee," *IEEE Trans. Power Syst.*, vol. 14, no. 3, pp. 1010–1020, Aug. 1999.

[54] M. Simab, M. S. Javadi, and A. E. Nezhad, "Multi-objective programming of pumped-hydro-thermal scheduling problem using normal boundary intersection and VIKOR," *Energy*, vol. 143, pp. 854–866, Jan. 2018.
[55] K. Hausken and J. Zhuang, *Game Theoretic Analysis of Congestion, Safety and Security*. Cham, Switzerland: Springer, 2015.

RAHEEL ZAFAR (Member, IEEE) received the B.Sc. and M.Sc. degrees in electrical engineering from the University of Engineering and Technology (UET), Lahore, in 2009 and 2011, respectively, and the Ph.D. degree in electrical engineering with specialization in power systems from the University of New South Wales (UNSW), Sydney, Australia, in 2019.

He worked as a Lecturer at UET Lahore for one and a half years. He worked as an Assistant Professor at the GIK Institute. He worked at industry for four years. He is currently working as an Assistant Professor with the Department of Electrical Engineering, Lahore University of Management Sciences (LUMS), Pakistan. His research interest includes the technical challenges involved in the integration of renewable energy sources into distribution grids.

ALI ESMAEEL NEZHAD (Graduate Student Member, IEEE) was born in Shiraz, Iran, in 1989. He received the B.Sc. and dual M.S. degrees in electrical engineering, in 2011, 2013, and 2020, respectively. He is currently a Junior Researcher in electrical engineering with LUT University, Finland. His current research interests include smart homes, energy hub, planning in restructured power systems, power market, plug-in electric vehicles, and renewable energy sources.

ABDOLLAH AHMADI (Member, IEEE) received the Ph.D. degree in electrical engineering from the University of New South Wales, Sydney, Australia, in 2019. He has authored or coauthored more than 85 international journal articles and book chapters. His research interests include renewable energy systems, smart grids, electricity markets, and power system operation and restructuring.

TOHID ERFANI is currently an Associate Professor with the UCL's Department of Civil and Environmental Engineering. He is interested in environmental resource management, green and sustainable planning, and water and energy infrastructure expansion under uncertainty. His research interests include developing optimization algorithms and mathematical models and applying system perspective approaches for sustainable, resilient, and efficient solution under extreme events. His work is funded by water companies, regulators, research institutes, and U.K. research councils, where he acts as a modeler and an adviser.

RASOOL ERFANI is currently a Senior Lecturer in fluid mechanics. His group contributes leading research in fundamental understanding of plasma engineering and experimental and computational fluid dynamics. He applies those knowledges in environmental science technological development for resource management and health care. His group works closely with other U.K. and international universities and various industries. He received the IMechE's Andrew Medd Award as the Winner of the Young Mechanical Engineer of the Year 2019/2020 for his contribution to the engineering science through community involvement and inspiring the next generation.